

How much Uranium is in the Earth?

Predictions for geo-neutrinos at KamLAND

Gianni Fiorentini,^{1,2,*} Marcello Lissia,^{3,4,†} Fabio
Mantovani,^{5,6,2,‡} and Riccardo Vannucci^{7,8,§}

¹*Dipartimento di Fisica, Università di Ferrara, I-44100 Ferrara, Italy*

²*Istituto Nazionale di Fisica Nucleare,
Sezione di Ferrara, I-44100 Ferrara, Italy*

³*Istituto Nazionale di Fisica Nucleare,
Sezione di Cagliari, I-09042 Monserrato, Italy*

⁴*Dipartimento di Fisica, Università di Cagliari, I-09042 Monserrato, Italy*

⁵*Dipartimento di Scienze della Terra,
Università di Siena, I-53100 Siena, Italy*

⁶*Centro di GeoTecnologie CGT, I-52027 San Giovanni Valdarno, Italy*

⁷*Dipartimento di Scienze della Terra,
Università di Pavia, I-53100 Siena, Italy*

⁸*Centro di GeoTecnologie CGT, I-27100 Pavia, Italy*

(Dated: January 4, 2005; revised July 19, 2005)

Abstract

Geo-neutrino detection can determine the amount of long-lived radioactive elements within our planet, thus providing a direct test of the Bulk Silicate Earth (BSE) model and fixing the radiogenic contribution to the terrestrial heat. We present a prediction for the geo-neutrino signal at KamLAND as a function of the Uranium mass in the Earth. The prediction is based on global mass balance, supplemented by a detailed geochemical and geophysical study of the region near the detector. The prediction is weakly dependent on mantle modeling. If BSE is correct, Uranium geo-neutrinos will produce between 25 and 35 events per year and 10^{32} protons at Kamioka.

PACS numbers: **check 91.35.-x, 13.15.+g, 14.60.Pq, 23.40.Bw**

*Electronic address: fiorenti@fe.infn.it

†Electronic address: marcello.lissia@ca.infn.it

‡Electronic address: mantovani@fe.infn.it

§Electronic address: vannucci@crystal.unipv.it

I. INTRODUCTION

The deepest hole that has ever been dug is about 12 Km deep, a mere dent in planetary terms. Geochemists analyze samples from the Earth’s crust and from the top of the mantle, whereas seismology can reconstruct the density profile throughout the whole Earth but not its composition. In this respect, our planet is mainly unexplored. Geo-neutrinos — the antineutrinos from the progenies of U, Th and ^{40}K decays in the Earth — bring to the surface information from the whole planet, concerning its content of radioactive elements. Their detection can shed light on the sources of the terrestrial heat flow, on the present composition and on the origins of the Earth.

Geo-neutrino properties, summarized in Table I, deserve a few comments:

(i) geo-neutrinos originating from different elements can be distinguished due to their different energy spectra, e.g., geo-neutrinos with energy $E > 2.25$ MeV are produced only from the Uranium chain;

(ii) geo-neutrinos from U and Th (not those from ^{40}K) are above threshold for the classical anti-neutrino detection reaction, the inverse beta on free protons:

$$\bar{\nu} + p \rightarrow e^+ + n - 1.8 \text{ MeV} \quad ; \quad (1)$$

(iii) anti-neutrinos from the Earth are not obscured by solar neutrinos, which cannot yield reaction (1).

TABLE I: The main properties of geo-neutrinos: ϵ_H is the heat production rate per unit mass and natural isotopic composition; $\epsilon_{\bar{\nu}}$ is the antineutrino production rate (number of antineutrinos per unit time) per unit mass (Contribution of ^{235}U is neglected due to the small, 0.7%, natural abundance).

Decay	Q	$\tau_{1/2}$	E_{max}	ϵ_H	$\epsilon_{\bar{\nu}}$
	[MeV]	[10^9 yr]	[MeV]	[W/Kg]	[$\text{kg}^{-1}\text{s}^{-1}$]
$^{238}\text{U} \rightarrow ^{206}\text{Pb} + 8\ ^4\text{He} + 6e + 6\bar{\nu}$	51.7	4.47	3.26	0.95×10^{-4}	7.41×10^7
$^{232}\text{Th} \rightarrow ^{208}\text{Pb} + 6\ ^4\text{He} + 4e + 4\bar{\nu}$	42.7	14.0	2.25	0.27×10^{-4}	1.63×10^7
$^{40}\text{K} \rightarrow ^{40}\text{Ca} + e + \bar{\nu}$	1.32	1.28	1.31	0.36×10^{-8}	2.69×10^4

Geo-neutrinos were introduced by Eder [1] in the sixties and Marx [2] soon realized their relevance. In the eighties Krauss et al. discussed their potential as probes of the Earth's interior in an extensive publication [3]. In the nineties the first paper on a geophysical journal was published by Kobayashi et al. [4]. In 1998, Raghavan et al. [5] and Rotschild et al. [6] pointed out the potential of KamLAND and Borexino for geo-neutrino detection.

In the last three years more papers appeared than in the previous decades: in a series of papers Fiorentini et al. [7, 8, 9, 10, 11] discussed the role of geo-neutrinos for determining the radiogenic contribution to the terrestrial heat flow and for discriminating among different models of Earth's composition and origin. A reference model for geo-neutrino production, based on a compositional map of the Earth's crust and on geochemical modeling of the mantle, was presented in [9]. At the end of 2002, the analysis of the first data release of KamLAND [12] (equivalent to an exposure of 0.11×10^{32} proton yr and 100% efficiency) reported 4 events from Uranium and 5 from Thorium out of a total of 32 counts in the geo-neutrino energy region ($E_{\text{vis}} < 2.6$ MeV), after subtracting 20 reactor events and 3 background counts. Statistical fluctuations imply an error of, at least, 5.7 counts. Indeed, this first indication of geo-neutrinos stimulated several investigations [13, 14, 15, 16, 17, 18, 19, 20].

In a few years KamLAND should provide definite evidence of geo-neutrino signal, after accumulating a much larger statistics and reducing background. In the meanwhile other projects for geo-neutrino detection are being developed. Borexino at Gran Sasso, which is expected to take data in a few years, will benefit from the absence of nearby reactors. Domogatski et al. [21] are proposing a 1 Kton scintillator detector in Baksan, again very far from nuclear reactors. A group at the Sudbury Neutrino Observatory in Canada is studying the possibility of using liquid scintillator after the physics program with heavy water is completed. The LENA proposal envisages a 30 Kton liquid scintillator detector at the Center for Underground Physics in the Pyhasälmi mine (Finland). Due to the huge mass, it should collect several hundreds of events per year. In conclusion, one can expect that within 10 years the geo-neutrino signal from Uranium and Thorium will be measured at a few points on the globe.

In this paper we shall concentrate on geo-neutrinos from Uranium, which are closer to experimental detection, and on the predictions for Kamioka, the site hosting the only detector which is presently operational. *Our goal is to understand which information on the*

total amount of Uranium in the Earth can be extracted from geo-neutrino measurements.

As briefly discussed in the next section, the Uranium mass in the Earth is estimated on the grounds of cosmo-chemical arguments, based on the compositional similarity between Earth and carbonaceous chondrites. Measurements of samples from the Earth's crust imply that the crust contains about one half of this global estimate, whereas the mantle — which should contain the rest — is practically unexplored in this respect. A direct determination of the Uranium mass in the globe is clearly an important test of the origins of the Earth. Furthermore, such a determination will also fix the radiogenic contribution to the terrestrial heat flow, which is a presently debated issue, see, e.g., Ref. [23]. Early estimates of the geo-neutrino signal and their connection with the global Uranium content are also reviewed at the end of Section II.

The geo-neutrino signal depends on the total Uranium mass m in the Earth and on the geochemical and geophysical properties of the region around the detector [7]. For KamLAND, we estimated [9] that about one half of the signal is originated within 200 km from the detector. This region, although containing a globally negligible amount of uranium, produces a large contribution to the signal as a consequence of its proximity to the detector. This contribution has to be determined on the grounds of a detailed geochemical and geophysical study of the region, if one wants to extract from the total signal the remaining part which carries the relevant information on m . The study of the region around Kamioka, including the possible effects of the subducting plates below the Japan Arc and a discussion of the contribution from of the Japan Sea, is presented in Section III.

The contribution from the rest of the world, discussed in Section IV, depends on the total mass of Uranium as well as on its distribution inside the Earth, since the closer is the source to the detector the larger is its contribution to the signal. For each value of m , we shall construct the distributions of Uranium abundances which provide the maximal and minimal signals, under the condition that they are consistent with geochemical and geophysical information on the globe. For the Earth's crust we shall use a $2^\circ \times 2^\circ$ map [25] which distinguishes several crustal layers and to each layer we shall assign minimal/maximal values for the Uranium mass abundances. According to geochemists, the rest of Uranium should be found in the mantle. Observational data for this reservoir are very poor, however it is generally believed that Uranium abundance increases with depth. The assumption *that abundance is spherically symmetrical and non decreasing with depth will be enough to*

provide rather tight bounds on the mantle contribution to the geo-neutrino signal. This will be further combined with the results for the crust.

We shall put together the pieces of the above analysis in Section V, where we present our main result in Fig. 1: a narrow band describes the predicted signal as a function of Earth’s total Uranium mass. We remark that the extremes of the band correspond to the whole range of uncertainty, which is estimated according to the following criteria: (i) for statistical errors we consider a $\pm 3\sigma$ interval; (ii) for systematic uncertainties of geochemical and geophysical parameters we determine an interval such as to cover all modern estimates which we found in the literature; (iii) independent errors are combined in quadrature.

On the grounds of Fig. 1 we discuss how the geo-neutrino signal can provide a direct test of a fundamental paradigm on the origins and composition of our planet.

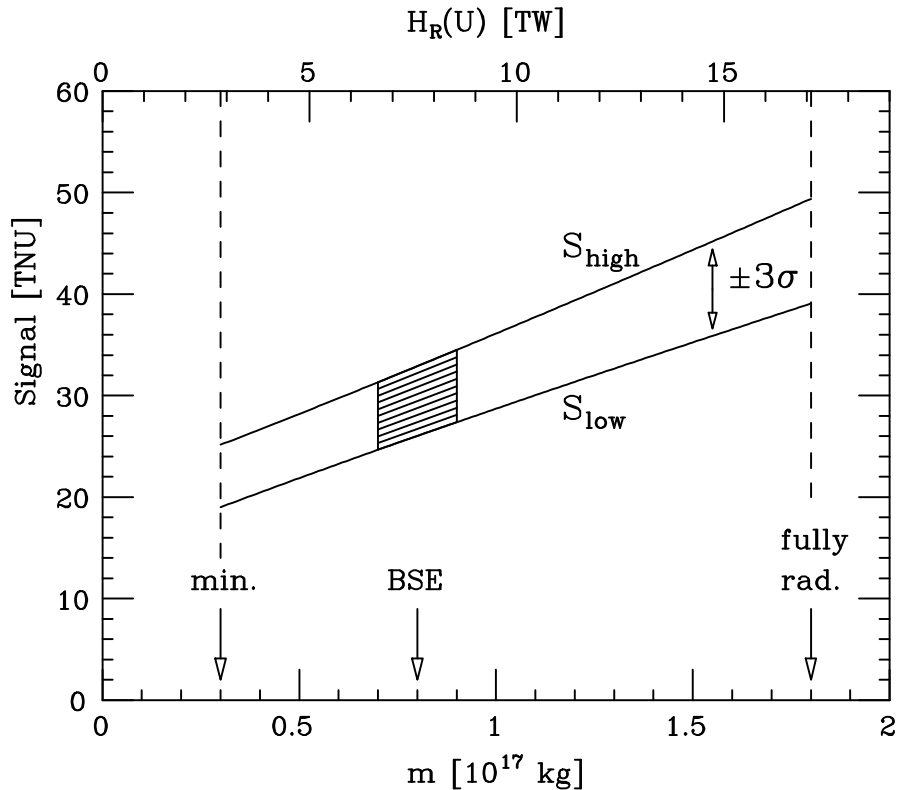


FIG. 1: The predicted signal from Uranium geo-neutrinos at KamLAND.

II. U, TH AND K IN THE EARTH: HOW MUCH AND WHERE?

Earth’s global composition is generally estimated from that of chondritic meteorites by using geochemical arguments which account for losses and fractionation during planet formation. Along these lines the Bulk Silicate Earth (BSE) model is built, which describes the “primitive mantle”, i.e., the outer portion of the Earth after core separation and before the differentiation between crust and mantle. The model is believed to describe the present crust plus mantle system. Since lithophile elements should be absent in the core ¹, the BSE provides the total amounts of U, Th and K in the Earth, estimates from different authors being concordant within 10-15% [26]. From the estimated masses, the present radiogenic heat production rate H_R and anti-neutrino luminosity $L_{\bar{\nu}}$ can be immediately calculated, see Table II and, e.g., Ref. [10].

TABLE II: U, Th and K according to BSE, from Ref. [10].

	m	H_R	L_{ν}
	[10^{17} kg]	[10^{12} W]	[10^{24} s ⁻¹]
U	0.8	7.6	5.9
Th	3.1	8.5	5.0
⁴⁰ K	0.8	3.3	21.6

The BSE is a fundamental geochemical paradigm. It is consistent with most observations, which however regard mostly the crust and an undetermined portion of the mantle. The measurement of quantities — such as the geo-neutrino signals — which are directly related to the global amounts of radioactive elements in the Earth will provide a direct test of this model for composition and origin of our planet.

For sure, heat released from radiogenic elements is a major source of the terrestrial heat flow, however its role is not understood at a quantitative level. The masses estimated within the BSE account for the present radiogenic production of 19 TW, which is about one

¹ One needs to be careful, since the definition of an element’s behavior, i.e., lithophile or not, depends on the surrounding system; there exist models of the Earth’s core suggesting it as repository for radioactive elements.

half of the estimated heat flow from Earth [23, 24]. Anderson refers to this difference as the missing heat source mystery and summarizes the situation with the following words: “Global heat flow estimates range from 30 to 44 TW ... Estimates of the radiogenic contribution ... based on cosmochemical considerations, vary from 19 to 31 TW. Thus, there is either a good balance between current input and output ... or there is a serious missing heat source problem, up to a deficit of 25 TW ...” If one can determine the amounts of radioactive elements by means of geo-neutrinos, an important ingredient of Earth’s energetics will be fixed.

Concerning the distribution of radiogenic elements, estimates for Uranium in the continental crust based on observational data are in the range:

$$m_C = (0.3 - 0.4) \times 10^{17} \text{ kg} \quad . \quad (2)$$

The extreme values have been obtained in Ref. [11] by taking the lowest (highest) concentration reported in the literature for each layer of the Earth’s crust, see Table II of Ref. [9], and integrating over a $2^\circ \times 2^\circ$ crust map. The main uncertainty is from the Uranium mass abundance a_{LC} in the lower crust, with estimates in the range (0.2 – 1.1) ppm. Estimates for the abundance in the upper crust, a_{UC} , are more concordant, ranging from 2.2 ppm to 2.8 ppm. The crust — really a tiny envelope — should thus contain about one half of the BSE prediction of Uranium in the Earth.

About the mantle, observational data are scarce and restricted to the uppermost part, so the best estimate for its Uranium content m_M is obtained by subtracting the crust contribution from the BSE estimate:

$$m_M = m_{\text{BSE}} - m_C \quad . \quad (3)$$

A commonly held view is that there is a vertical gradient in the abundances of incompatible elements in the mantle, with the top being most depleted. A minimum gradient model has a fully mixed and globally homogeneous mantle; the other extreme is a model where all the Uranium is at the bottom of the mantle.

Geochemical arguments are against the presence of radioactive elements in the completely unexplored core, as discussed by McDonough in a recent review of compositional models of the Earth [26].

Similar considerations hold for Thorium and Potassium, the relative mass abundance with respect to Uranium being globally estimated as:

$$a(\text{Th}) : a(\text{U}) : a(\text{K}) \approx 4 : 1 : 10,000 \quad . \quad (4)$$

We remark that the well-fixed ratios in Eq. (4) imply that detection of geo-neutrinos from Uranium will also bring important information on the amount of Thorium and Potassium in the whole Earth.

Several predictions for the geo-neutrino signal have been presented in the past, corresponding to different hypotheses about the amount of Uranium in the Earth and to different models of its distribution. A summary is presented in Fig. 2. Early models [1, 2, 4] (full circles) assumed a uniform Uranium distribution in the Earth and different values of the Uranium mass. In fact these predictions are almost proportional to m . The huge signals predicted by Eder and by Marx were obtained by assuming that the Uranium density in the whole Earth is about the same as that observed in the continental crust; Marx (Eder ²) assumed thus an Uranium mass 30 (60) times larger than that estimated within the BSE.

Krauss et al. [3] distributed about 10^{17} kg of Uranium uniformly over a 30 km crust. The other estimates (crosses) are all obtained by using the BSE value for the mass as an input and different models for distributing the Uranium content between crust and mantle. In this class, Rotschild et al. [6] obtained the minimal prediction by assuming for the crust a very small Uranium abundance, definitely lower than the values reported in more recent and detailed estimates.

In this paper we shall use a rather general approach, by keeping the total amount of Uranium as a free variable, within the loose constraints provided from one side by the amount observed in the crust and from the other side by the amount tolerated by Earth's energetics. We shall distribute the total amount between crust and mantle so as to maximize or minimize the signal, within the boundary provided by geochemical and/or geophysical observations.

² The factor 10.7 appearing in the last of the equations (13) of Ref. [1] should actually be 1.07 and, correspondingly, the reaction rate on page 661 has been divided by a factor of 10.

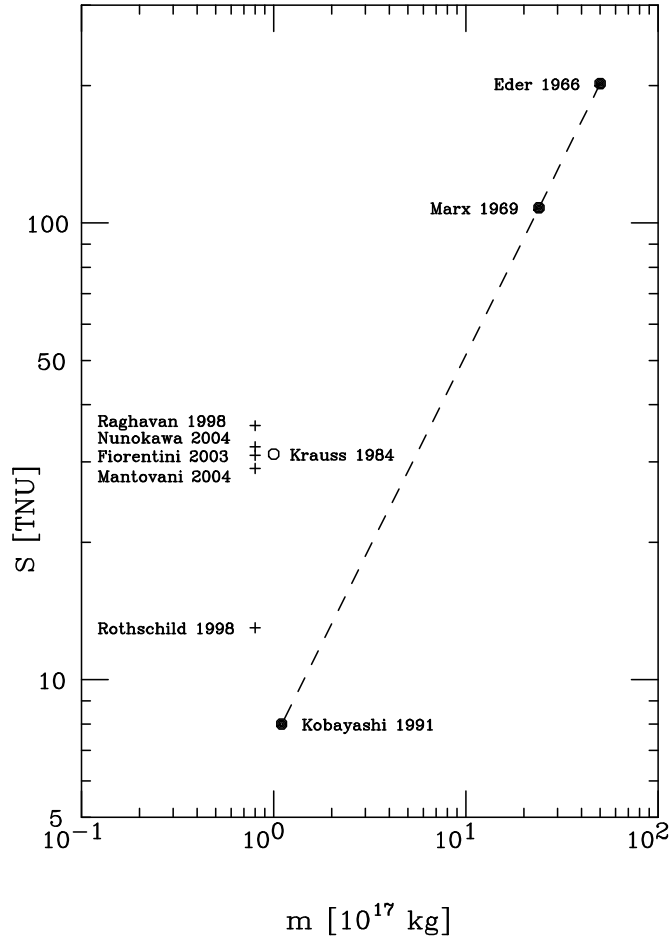


FIG. 2: Previous estimates of the geo-neutrino signal S , renormalized to the average survival probability $\langle P_{ee} \rangle = 0.59$, and the corresponding estimated Uranium mass m . The signal is in Terrestrial Neutrino Units (1 TNU = 1 event/year/ 10^{32} proton).

III. THE REGION NEAR THE DETECTOR

As mentioned in the introduction, the entire Earth's crust will be subdivided into $2^\circ \times 2^\circ$ tiles. Within each tile, one distinguishes several vertical layers and assigns to each layer a world averaged Uranium mass abundance, see Ref. [9]. With the aim of reducing the error on the regional contribution to the level of the uncertainty on the rest of the world, one

needs a more detailed geochemical and geophysical study of the crust in the region within a few hundreds kilometers from the detector, where some half of the signal is generated.

We shall present here our results for the region near the KamLAND detector, located at $36^{\circ} 25' 26''$ N and $137^{\circ} 19' 11''$ E. We analyze the six tiles (see Fig. 3) around KamLAND by using geochemical information on a $1/4^{\circ} \times 1/4^{\circ}$ grid and a detailed map of the crust depth. The possible (minimal and maximal) effects of the subducting slab beneath Japan are also considered and the uncertainty arising from the debated (continental or oceanic) nature of the crust below the Japan Sea is taken into account.

A. The six tiles near KamLAND

The seismic velocity structure of the crust beneath the Japan Islands has been determined in Ref. [27] from the study of some 13,000 arrival times of 562 local shallow earthquakes. By applying an inversion method, the depth distribution of the Conrad and Moho discontinuities beneath the whole of the Japan Islands are derived, with an estimated standard error of ± 1 km over most of Japan territory. Our Figs. 3 and 4 are derived from Fig. 6 of Ref. [27]. This allows distinguishing two layers in the crust: an upper crust extending down to the Conrad and a lower part down to the Moho discontinuity.

The upper-crust chemical composition of Japan Islands has been studied in Ref. [28], based on 166 representative specimens, which can be associated with 37 geological groups based on ages, lithologies and provinces. By combining the base geological map of Fig. 2 of Ref. [28] — which distinguishes 10 geological classes — with the abundances reported in Table 1 of the same paper, one can build a map of Uranium abundance in the upper crust, under the *important* assumption that the composition of the whole upper crust is the same as that inferred in Ref. [28] from the study of the exposed portion, see Fig. 5.

We are not aware of a specific study of the lower part of the Japan crust, however, it is well known that there are similarities between the composition of the Japanese crust and that of the Sino-Korean block. In an extensive compositional study of East China crust [29], the Uranium abundance in the lower part is estimated between 0.63 and 1.08 ppm. On these grounds we shall take for the abundance in the lower crust of Japan:

$$a_{LC} = 0.85 \pm 0.23 \quad . \quad (5)$$

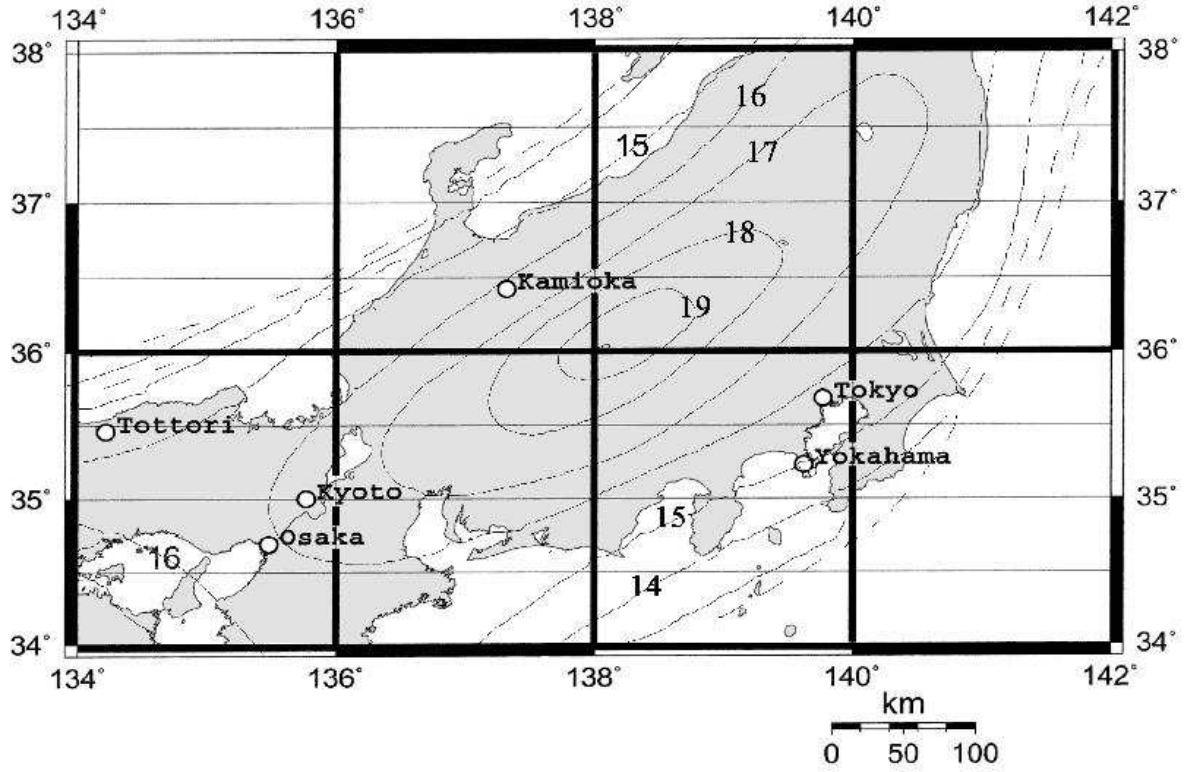


FIG. 3: Depth of the Conrad discontinuity in Japan, from Ref. [27].

We remark that the estimated range of abundances for East China is substantially narrower than the range for the whole world, which is (0.2-1.1) ppm (see Table II in Ref. [9]), this last interval presumably reflecting regional differences in the lower crust composition.

Concerning the vertical distribution of abundances in the crust, it is presently impossible to have information on the chemical composition on a scale smaller than the Conrad depth, generally lying at about 20 km. We also note that the sampling density for the study of the upper crust in the region near Kamioka is about one specimen per 400 km². On these grounds, we introduce a grid where one assigns a specific abundance to *cells* with size $1/4^\circ \times 1/4^\circ$, i.e., with a linear scale of about 20 km. Within each cell, the depth of the upper and lower crust are taken from Ref. [27], Uranium abundance for the upper crust is derived from Ref. [28] and for the lower crust from Ref. [29]. In this way each of the six tiles near Kamioka is subdivided into sixty-four cells.

Just for the sake of computing flux and signal, each cell is further subdivided into many *subcells* with abundance derived from those of the parent cell. The angle-integrated produced

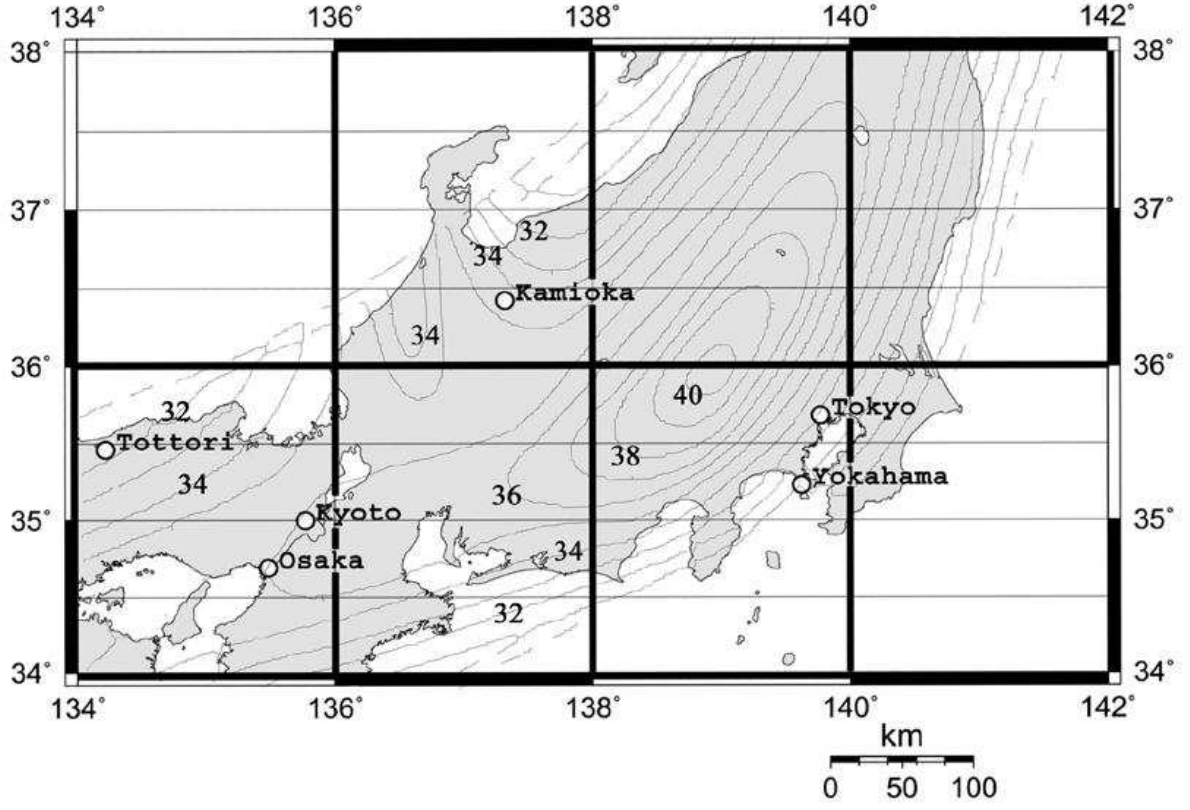


FIG. 4: Depth of the Moho discontinuity in Japan, from Ref. [27].

flux at distance R from a subcell of volume ΔV , calculated as that from a sphere with radius $r = (3/4\pi\Delta V)^{1/3}$, is

$$\Delta\Phi = \frac{A}{4R} \left[2Rr + (R^2 - r^2) \ln \frac{|R - r|}{R + r} \right] \quad , \quad (6)$$

where A is the specific activity (number of neutrinos produced per unit time and volume). Each subcell provides a contribution to the signal rate ΔS given by:

$$\Delta S = N_p \Delta\Phi \langle \sigma P_{ee}(R) \rangle \quad , \quad (7)$$

where N_p is the number of free protons in the target, σ is the cross section of reaction in Eq. (1), $P_{ee}(R)$ is the survival probability which we shall calculate for $\tan^2 \theta = 0.40$ and $\Delta m^2 = 7.9 \times 10^{-5} \text{ eV}^2$ [30]. The average is over the energy spectrum of the neutrinos from Uranium decay chain.

The resulting signal is obtained by adding the contributions of all subcells and will be expressed in Terrestrial Neutrino Units (TNU), where 1 TNU corresponds to 1 event per

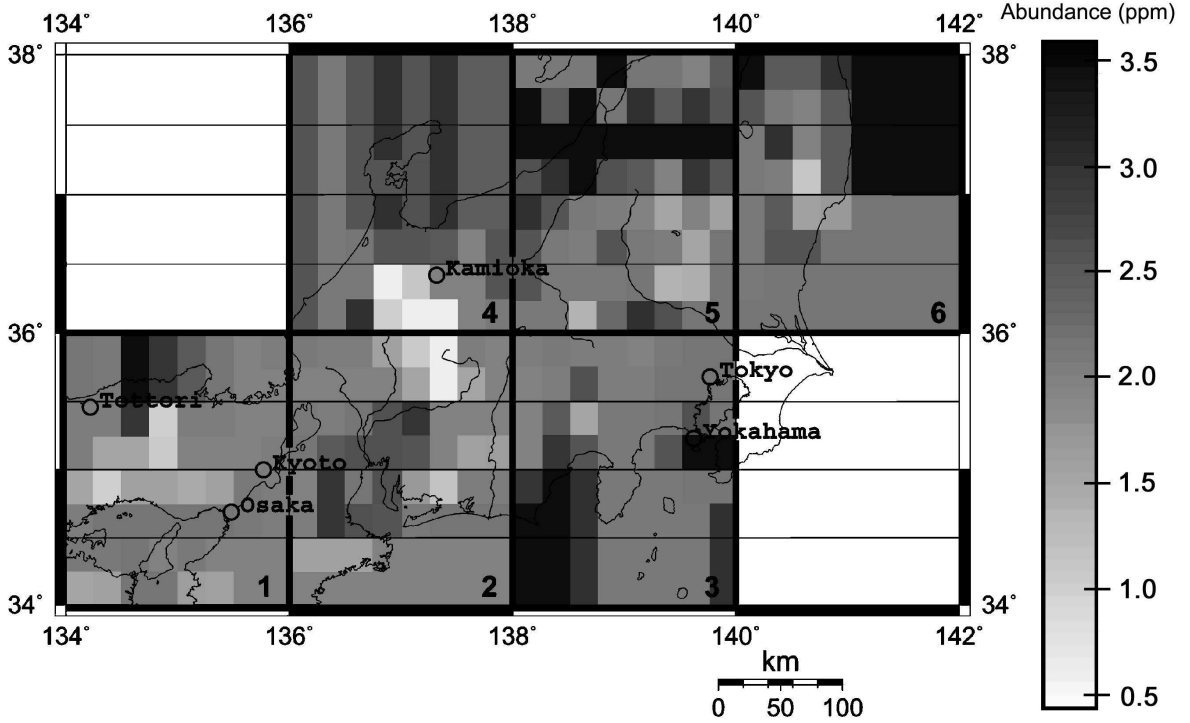


FIG. 5: Uranium abundance in the upper crust of Japan

year and per 10^{32} protons. The contributions to the produced flux and to the signal from the six tiles are:

$$\Phi_6 = 1.59 \times 10^6 \text{ cm}^{-2}\text{s}^{-1} \quad ; \quad (8a)$$

$$S_6 = 12.74 \text{ TNU} \quad . \quad (8b)$$

With respect to our previous estimate from the whole globe [9], giving $\Phi = 3.676 \times 10^6 \text{ cm}^{-2} \text{ s}^{-1}$ and $S = 28.6 \text{ TNU}$ for $\langle P_{ee} \rangle = 0.59$, we find that the six tiles contribute 43% of the flux and 45% of the signal: this justifies the close scrutiny of the region within the six tiles. Some 3/4 of the contribution arises from the upper crust.

In more detail, the tile hosting Kamioka generates 29% and 30% of the total produced flux and signal, respectively. The host cell, i.e., the cell where Kamioka is located, contributes 9% to the total produced flux.

The Uranium mass contained in the six tiles is about $m_6 = 3.3 \times 10^{13} \text{ kg}$, really negligible (less than 0.05%) with respect to that estimated for the whole Earth.

We have considered several sources of the uncertainties affecting this estimate, see Table III:

(i) *Measurement errors of the chemical analysis.* The standard error of the Uranium abundance measurements in the individual samples is 3-4% [28]. We translated this error into a $\pm 10\%$ global uncertainty (correspondingly to about 3σ) on the Uranium abundance in the upper crust for the six tiles ³.

(ii) *Discretization of the upper crust.* As mentioned above, we divided the crust into $1/4^\circ \times 1/4^\circ$ cells, assigning specific abundances to each cell. This discretization procedure introduces some uncertainty, which is especially important in the region very close to the detector. We have evaluated the effect of replacing the abundance of the host cell with those of adjacent cells. This produces signal variations in the interval $(-0.64, +1.68)$ TNU. For simplicity, we introduce a symmetrical error such as to encompass the extreme values.

(iii) *Chemical composition of the lower crust.* The error is taken as the half-difference between signals obtained for the extreme values of the estimated Uranium abundances in the lower crust.

(iv) *Crustal depth.* Since the depths of the Conrad and the Moho discontinuities are estimated with an 3σ accuracy of about ± 3 km, we have evaluated the effect of such (global) variations over the six tiles, the error being again estimated as the half difference between extreme values of flux/signal.

TABLE III: Errors from the regional geophysical and geochemical uncertainties.

Source	ΔS (TNU)	Remarks
Composition of upper-crust samples	0.96	3σ error
Upper-crust discretizaion	1.68	
Lower-crust composition	0.82	Full range
Crustal depths	0.72	3σ error
Subducting slab	2.10	Full range
Japan Sea	0.31	Full Range
Total	3.07	

³ This choice is very conservative given our lack of information on the correlation between the errors of the 166 samples: the errors should partially average out and result in a total error between 12% and $(12/\sqrt{166})\% \approx 1\%$.

B. The effect of the subducting slab beneath Japan

The Japan arc, at the crossing among the Eurasian, Philippine and Pacific plates, is the theater of important subduction processes. The Philippine plate is moving towards the Eurasia plate at about 40 mm/yr and is subducting beneath the southern part of Japan. The Pacific Plate is moving in roughly the same direction at about 80 mm/yr and is subducting beneath the northern half of Japan.

We shall model these processes as a single slab penetrating below Japan with velocity $v = 60$ mm/yr, the average of the two plates. This process has been occurring on a time scale $T \approx 10^8$ y, during which the front has advanced by $D = vT \approx 6000$ km.

We assume that the slab brings with it a sediments layer (with density $\rho_{\text{sed}} \approx 1.6$ ton/m³, depth $h_{\text{sed}} \approx 350$ m and Uranium abundance $a_{\text{sed}} = 1.4$ ppm, according to the data for the Japan trench [31]) on top of an oceanic crust layer, with density $\rho_{OC} \approx 2.9$ ton/m³, vertical extension $h_{OC} \approx 6.5$ km, and Uranium abundance $a_{OC} = 0.1$ ppm.

The amount of Uranium carried by the slab per unit surface is thus:

$$\sigma_{\text{slab}} = a_{\text{sed}} \times \rho_{\text{sed}} \times h_{\text{sed}} + a_{OC} \times \rho_{OC} \times h_{OC} = 2.7 \text{ kg/m}^2 \quad . \quad (9)$$

We observe that the corresponding quantity for the lower continental crust of Japan (density $\rho_{LC} \approx 2.7$ ton/m³, average depth $h_{LC} \approx 19$ km, and Uranium abundance $a_{LC} = 0.85$ ppm) is:

$$\sigma_{LC} = a_{LC} \times \rho_{LC} \times h_{LC} = 43.6 \text{ kg/m}^2 \quad . \quad (10)$$

In order to estimate the effect of the subducting slab on geo-neutrino production, one can envisage two extreme cases:

(a) one assumes that the slab keeps its trace elements while subducting. The effect of its presence can be estimated as if the lower crust is effectively enriched by the amount of Uranium contained in the crustal part of the slab passing below it, i.e., $\sigma_{LC} \rightarrow \sigma_{LC} + \sigma_{\text{slab}}$, a negligible effect in comparison with the 25% uncertainty on σ_{LC} resulting from $\Delta a_{LC} \approx 0.2$ ppm. The signal is increased by 0.2 TNU.

(b) At the other extreme, it is possible that, as the slab advances, *all* Uranium from the subducting crust is dissolved in fluids during dehydration reactions and accumulates in the lower part of the continental crust of Japan, thus strongly enriching it. The release process — to a first approximation — will be uniform along the subduction direction, for

some distance $d \approx 250$ km corresponding to the dimension of the Japan arc transverse to the trench. Since the slab has advanced by $D \approx 6000$ km, the abundance increase in the lower crust is now:

$$\delta\sigma_{LC} = \sigma_{\text{slab}} \times \frac{D}{d} \approx 68.4 \text{ kg/m}^2 \quad . \quad (11)$$

This corresponds to a substantial increase of the effective Uranium abundance in the Japanese lower continental crust. The signal contributed from the lower crust of Japan increases by 4.4 TNU.

As we have no argument for deciding which of the extreme cases (a) or (b) is closer to reality and in order to encompass both of them, we estimate the contribution from the subducting slab as:

$$S_{\text{slab}} = (2.3 \pm 2.1) \text{ TNU} \quad . \quad (12)$$

C. The crust below the Japan Sea

The morphology of the Japan Sea, characterized by three major basins (Japan, Yamato, and Ulleung Basins) and topographic highs such as the Yamato Ridge, is suggestive of intricate back-arc opening tectonics. Based on seismic reflection/refraction survey data, bottom sampling data, geomagnetic data and basement depth and topography, Tamaki et al. [32] distinguish four crustal types: continental, rifted continental, extended continental, and oceanic crust. The Japan basin is generally considered as oceanic, whereas the nature of other basins is controversial and debated. Again, we resort to two extreme models:

(a) following Ref. [25] we consider all the basins as formed with oceanic crust, extending down to 7 km below 1 km of sediments. This provides a model for minimal geo-neutrino production, resulting in $S_{JS} = 0.06$ TNU.

(b) Deeper crustal depths (up to 19 km for the Oki bank) and thicker sediments layers (up to 4 km for the Ulleung basin) are reported in the literature, see Table IV. By taking these values and assigning the abundances typical of continental crust, we maximize geo-neutrino production, with the result $S_{JS} = 0.68$ TNU.

In between (a) and (b), and in order to encompass the extreme values, we fix the contribution to the signal from the Japan Sea as:

$$S_{JS} = (0.37 \pm 0.31) \text{ TNU} \quad . \quad (13)$$

TABLE IV: The vertical extensions (km) of crustal layers in the Yamano basin (YB), Oki bank (OK), and Ulleung basin (UB) used for model (b).

	YB	OK	UB
sediments	1.2	0.3	4
upper	2.8	8.7	2
lower	8.5	10.5	8

D. Summary of the regional contribution

The regional contribution to the signal can be determined by adding the previous results. As the errors are independent, we combine them in quadrature, obtaining:

$$S_{\text{reg}} = (15.41 \pm 3.07) \text{ TNU} \quad . \quad (14)$$

The principal uncertainty comes from the effect of the subducting slab. A more detailed study of the mechanisms of Uranium release should exclude the extreme cases which we have considered, thus reducing the error.

Discretization of the crust is major uncertainty. A more detailed description of the exposed crust is certainly achievable, however, it will bring little help without a better understanding of the chemical composition variation with depth.

IV. THE REST OF THE WORLD

The contribution from the rest of the world will depend on the total mass of Uranium m as well as on its distribution inside the Earth, since the closer is the source to the detector the larger is its contribution to the signal. For each value of m , we shall construct the distributions which provide the maximal and minimal signals under the condition that they are consistent with geochemical and geophysical information on the globe.

For the Earth's crust, we use the $2^\circ \times 2^\circ$ map of Ref. [25] distinguishing several crustal layers which are known to contain different amounts of radioactive elements. For each layer minimal and maximal estimates of Uranium abundances found in the literature are adopted, so as to obtain a range of acceptable fluxes, see Table V.

TABLE V: Minimal and maximal estimated Uranium abundances for the continental crust, in ppm.

	min	max
upper crust	2.2	2.8
lower crust	0.2	1.1

Depending on the adopted values, the Uranium mass in the crust m_C is the range (0.3 – 0.4) in units — here and in the following — of 10^{17} kg. Clearly the larger is the mass the bigger is the signal, the extreme values being ⁴:

$$S_C^{(\min)} = 6.448 \quad \text{for } m = 0.3 \quad \text{and} \quad S_C^{(\max)} = 8.652 \quad \text{for } m = 0.4. \quad (15)$$

Concerning Uranium in the mantle, we assume that spherical symmetry holds and that the Uranium mass abundance is a non-decreasing function of depth. It follows that, for a fixed Uranium mass in the mantle m_M , the extreme predictions for the signal are obtained by: (i) placing Uranium in a thin layer at the bottom and (ii) distributing it with uniform abundance over the mantle. These two cases give, respectively:

$$S_M^{(\min)} = 12.15 \times m_M \text{ TNU} \quad \text{and} \quad S_M^{(\max)} = 17.37 \times m_M \text{ TNU}. \quad (16)$$

By using again the proximity argument, we can combine the contributions from crust and mantle so as to obtain extreme predictions: for a fixed total $m = m_C + m_M$, the highest signal is obtained by assigning to the crust as much material as consistent with observational data ($m_C = 0.4$) and putting the rest, $m - m_C$, in the mantle with a uniform distribution. Similarly, the minimal flux/signal is obtained for the minimal mass in the crust ($m_C = 0.3$) and the rest in a thin layer at the bottom of the mantle. In conclusion, the contribution from the rest of the world is in the range:

$$S_{RW}^{(\min)} = [6.448 + 12.15(m - 0.3)] \text{ TNU} \quad \text{and} \quad S_{RW}^{(\max)} = [8.652 + 17.37(m - 0.4)] \text{ TNU}. \quad (17)$$

⁴ As we are now considering distances from the detector which are considerably larger than the neutrino oscillation length, the asymptotic expression for the survival probability, $\langle P_{ee} \rangle = (1 - 1/2 \sin^2(2\theta)) = (1 + \tan^4 \theta)/(1 + \tan^2 \theta)^2$ holds, so that the produced flux and signal are directly proportional, $S/\text{TNU} = 13.2 \times \langle P_{ee} \rangle \Phi / (10^6 \text{ cm}^{-2} \text{ s}^{-1})$ [8].

Note that the two straight lines cross near $m = 0.21$, i.e., in the nonphysical region, since Uranium mass is at least 0.3.

We remind that both the Uranium poor ($m_C = 0.3$) and the Uranium rich ($m_C = 0.4$) crust models are observationally acceptable. We also recall that a compositionally uniform mantle is advocated by geophysicists, whereas geochemists prefer a two-layered mantle with a lower part close to the primitive composition and an upper part strongly impoverished in Uranium. In other words, it seems to us that the extreme predictions correspond to equally plausible models. On these grounds, we take as our prediction the mean of the extremes and assign an error so as to encompass both of them:

$$S_{RW} = [(2.25 + 14.76 \times m) \pm (-0.55 + 2.61 \times m)] \text{ TNU} \quad . \quad (18)$$

We remark that by combining global mass balance with geometry, we have strongly constrained the contribution from the rest of the world: for a mass near the BSE values, $m \approx 0.8$, the signal is predicted within about 10%.

V. THE GEO-NEUTRINO SIGNAL AS A FUNCTION OF URANIUM MASS IN THE EARTH

By combining the regional contribution, Eq. (14), with that from the rest of the world, Eq. (18), we get the Uranium geo-neutrino signal as a function of Uranium mass in the Earth:

$$S = S_0 \pm \Delta \quad , \quad (19a)$$

where:

$$S_0 = 17.66 + 14.76 \times m \quad (19b)$$

$$\Delta^2 = (3.07)^2 + (2.61 \times m - 0.55)^2 \quad . \quad (19c)$$

This error is obtained by combining in quadrature all geochemical and geophysical uncertainties discussed in the preceding paragraphs. All of them have been estimated so as to cover $\pm 3\sigma$ intervals of experimental measurements and total ranges of theoretical predictions.

However, this error does not account for present uncertainties on neutrino oscillation parameters and on the cross section of reaction in Eq. (1). For the sake of discussing the potential of geo-neutrinos, we shall ignore for the moment these error sources.

The expected signal from Uranium geo-neutrinos at KamLAND is presented as a function of the total Uranium mass m in Fig. 1. The upper horizontal scale indicates the corresponding radiogenic heat production rate from Uranium ($H_R = 9.5 \times m$).

The predicted signal as a function of m is between the two lines denoted as S_{high} and S_{low} , which correspond, respectively, to $S_0 \pm \Delta$.

Since the minimal amount of Uranium in the Earth is 0.3×10^{17} kg (corresponding to the minimal estimate for the crust and the assumption of negligible amount in the mantle), we expect a signal of at least 19 TNU. On the other hand, the maximal amount of Uranium tolerated by Earth’s energetics ⁵, 1.8×10^{17} kg, implies a signal not exceeding 49 TNU.

For the central value of the BSE model, $m = 0.8 \times 10^{17}$ kg, we predict $S = 29.5 \pm 3.4$ TNU, i.e., with an accuracy of 12% at “ 3σ ”. We remark that estimates by different authors for the Uranium mass within the BSE are all between $(0.7 - 0.9) \times 10^{17}$ kg. This implies that the Uranium signal has to be in the interval $(24.7 - 34.5)$ TNU. The measurement of geo-neutrinos can thus provide a direct test of an important geochemical paradigm.

The effect of uncertainties about the oscillation parameters is presented in Table VI. In this respect the mixing angle is most important. Figure 4 (b) of Ref. [30] shows a 3σ range $0.26 < \tan^2 \theta < 0.67$ (central value 0.40): the corresponding range for the average survival probability is $0.52 < P_{ee} < 0.67$ (central value 0.59), with a 3σ relative error on the signal $\Delta S/S \approx 13\%$, which is comparable to the geological uncertainty in Eq. (19c). The mixing angle should be determined more precisely for fully exploiting the geo-neutrino signal.

On the other hand, the predicted signal is practically unaffected by the uncertainty on the neutrinos squared mass difference δm^2 : when this is varied within its $\pm 3\sigma$ interval the signal changes by 0.1 TNU. This holds for any value of the total Uranium mass m , since the precise value of δm^2 only matters in the region near the detector. In addition, we observe that the predictions computed for the best value ($\delta m^2 = 7.9 \times 10^{-5}$ eV²) and for the limit $\delta m^2 = \infty$ differ by +0.3 TNU. Finally, the error on the inverse-beta cross section (quoted

⁵ For an Uranium mass $m = 1.8 \times 10^{17}$ kg and relative abundances as in Eq. (4), the present radiogenic heat production rate from U, Th and K decays equals the maximal estimate for the present heat flow from Earth, $H_E^{\text{max}} = 44$ TW [22].

TABLE VI: Effect of the oscillation parameters on the signal. The relative/absolute variation is computed with respect to the prediction for the best fit values ($\delta m^2 = 7.9 \times 10^{-5} \text{ eV}^2$ and $\tan^2 \theta = 0.40$).

parameter	signal variation
$\tan^2 \theta = 0.26$	+13.5%
$\tan^2 \theta = 0.67$	-12.2%
$\delta m^2 = 6.9 \times 10^{-5} \text{ eV}^2$	+0.11 TNU
$\delta m^2 = 9.3 \times 10^{-5} \text{ eV}^2$	-0.10 TNU

as 0.2% at 1σ in Ref. [12]) translates into a 3σ uncertainty of 0.6% on the signal.

VI. CONCLUDING REMARKS

We summarize here the main points of this paper:

(1) Based on a detailed geochemical and geophysical study of the region near Kamioka, we have determined the regional contribution to the signal from Uranium-geoneutrinos:

$$S_{\text{reg}} = (15.41 \pm 2.98) \text{ TNU} \quad . \quad (20)$$

(2) By using global mass balance arguments, we have determined the contribution from the rest of the world:

$$S_{RW} = [(2.25 + 14.76 \times m) \pm (-0.55 + 2.61 \times m)] \text{ TNU} \quad , \quad (21)$$

where m is the Uranium mass in the Earth, in units of 10^{17} kg .

(3) Our prediction for the signal as a function of m is presented in Fig. 1, which shows the potential of geo-neutrinos for determining how much Uranium is in the Earth (As discussed in the paper, the range of the prediction for a given mass is mostly due to experimental determinations of local abundances and to the geometrical distributions of trace elements in the mantle).

(4) Measurements of the antineutrino signal from Uranium can provide crucial tests for models. In particular, estimates by different authors for the Uranium mass within the

important paradigm of the Bulk Silicate Earth are all in the range $(0.7, 0.9) \times 10^{17}$ kg, which translates into a signal $23 < S(U) < 31$ TNU.

(5) A full exploitation of the geo-neutrino signal demands that the mixing angle is determined more precisely.

Acknowledgments

We are particularly grateful to Enomoto Sanshiro for useful discussions and for pointing to our attention Refs. [27] and [28]. We thank M. Contorti, K. Inoue, and E. Lisi for valuable comments. The final manuscript includes several useful remarks by the anonymous referees.

This work was partially supported by MIUR (Ministero dell’Istruzione, dell’Università e della Ricerca) under MIUR-PRIN-2003 project “Theoretical Physics of the Nucleus and the Many-Body Systems” and MIUR-PRIN-2004 project “Astroparticle physics”.

Note added in Proofs

The KamLAND collaboration has just presented experimental results [33] on geo-neutrinos, which are in agreement with our predictions, see Ref. [34] for a comparison.

-
- [1] G. Eder, Nucl. Phys. **78**, 657 (1966).
 - [2] G. Marx, Czech. J. Phys. **B 19**, 1471-1479 (1969).
 - [3] L. M. Krauss, S. L. Glashow, and D. N. Schramm, Nature (London) **310**, 191 (1984).
 - [4] M. Kobayashi and Y. Fukao, Geophysical Research Lett. **18**, 633-636 (1991).
 - [5] R. S. Raghavan, S. Schönert, S. Enomoto, J. Shirai, F. Suekane, and A. Suzuki, Phys. Rev. Lett. **80**, 635 (1998).
 - [6] C. G. Rothschild, M. C. Chen, and F. P. Calaprice, Geophys. Res. Lett. **25**, 1083 (1998) [arXiv:nucl-ex/9710001].
 - [7] G. Fiorentini, F. Mantovani, and B. Ricci, Phys. Lett. B **557**, 139 (2003) [arXiv:nucl-ex/0212008].
 - [8] G. Fiorentini, T. Lasserre, M. Lissia, B. Ricci, and S. Schönert, Phys. Lett. B **558**, 15 (2003) [arXiv:hep-ph/0301042].

- [9] F. Mantovani, L. Carmignani, G. Fiorentini and M. Lissia, Phys. Rev. D **69**, 013001 (2004) [arXiv:hep-ph/0309013].
- [10] G. Fiorentini, M. Lissia, F. Mantovani and R. Vannucci, arXiv:hep-ph/0409152.
- [11] G. Fiorentini, M. Lissia, F. Mantovani and R. Vannucci, Astroparticle and high energy physics AHEP2003/035 [arXiv:hep-ph/0401085].
- [12] KamLAND Collaboration, K. Eguchi *et al.*, Phys. Rev. Lett. **90**, 021802 (2003) [arXiv:hep-ex/0212021].
- [13] H. Nunokawa, W. J. C. Teves and R. Zukanovich Funchal, JHEP **0311**, 020 (2003) [arXiv:hep-ph/0308175].
- [14] T. Mitsui [KamLAND Collaboration], *Proceedings of the 28th International Cosmic Ray Conferences (ICRC 2003), Tsukuba, Japan, 31 Jul - 7 Aug 2003*, pp. 1221-1224.
- [15] L. Miramonti, arXiv:hep-ex/0307029.
- [16] G. Domogatski, V. Kopeikin, L. Mikaelyan and V. Sinev, arXiv:hep-ph/0401221.
- [17] R. D. McKeown and P. Vogel, Phys. Rept. **394**, 315 (2004) [arXiv:hep-ph/0402025].
- [18] B. D. Fields and K. A. Hochmuth, arXiv:hep-ph/0406001.
- [19] V. D. Rusov, V. N. Pavlovich, V. N. Vaschenko, V. A. Tarasov, D. A. Litvinov, V. N. Bolshakov and E. N. Khotyaintseva, arXiv:hep-ph/0312296.
- [20] G. L. Fogli, E. Lisi, A. Palazzo and A. M. Rotunno, arXiv:hep-ph/0405139.
- [21] G. Domogatski, V. Kopeikin, L. Mikaelyan and V. Sinev, arXiv:hep-ph/0409069.
- [22] H. N. Pollack, S. J. Hunter and J. R. Johnson, Rev. Geophys. **31**, 267-280 (1993).
- [23] D. Anderson, Energetics of the Earth and the Missing Heat Source Mystery, available at www.mantleplumes.org/Energetics.html
- [24] A. M. Hofmeister and R. E. Criss, Tectonophysics **395**, 159–177 (2005).
- [25] C. Bassin, G. Laske. and G. Masters, EOS Trans. Am. Geophys. Union **81**, F897 (2000) [<http://mahi.ucsd.edu/Gabi/rem.html>].
- [26] W. F. McDonough, Compositional Model for The Earth's Core, pp. 547-568. In The Mantle and Core (ed. R.W. Carlson.) Vol. 2 Treatise on Geochemistry (eds. H.D. Holland and K.K. Turekian), Elsevier-Pergamon, Oxford (2003).
- [27] D. Zhao, S. Horiuchi and A. Hasegawa, Tectonophysics **212**, 289-301 (1992).
- [28] S. Togashi, et al., Geochem. Geophys. Geosyst. (Electronic Journal of the Earth Sciences) **1**, 2000GC00083 (2000).

- [29] S. Gao, et al., *Geochimica et Cosmochimica Acta* **62**, 1959-1975 (1998).
- [30] T. Araki *et al.* [KamLAND Collaboration], arXiv:hep-ex/0406035.
- [31] T. Plank and C. H. Langmuir, *Chemical geology* **145**, 325-394 (1998).
- [32] K. Tamaki, K. Suyehiro, J. Allan, J. C. Ingle, and K. A. Pisciotto, in *Proc. ODP, Sci. Results*, edited by K. Tamaki, K. Suyehiro, J. Allan, M. McWilliams, et al., **127/128**, 1333-1348, College Station, TX (Ocean Drilling TAMU), (1992).
- [33] T. Araki *et al.* [KamLAND Collaboration], *Nature* **436**, 499 (2005).
- [34] G. Fiorentini, M. Lissia, F. Mantovani and B. Ricci, arXiv:hep-ph/0508048.